

## Research Article



# Evaluation of the periodontal regenerative properties of patterned human periodontal ligament stem cell sheets

Joong-Hyun Kim <sup>1</sup>, Seok-Yeong Ko <sup>1</sup>, Justin Ho Lee <sup>2</sup>, Deok-Ho Kim <sup>2,3,4</sup>,  
Jeong-Ho Yun <sup>1,5,6,\*</sup>

<sup>1</sup>Department of Periodontology, Chonbuk National University School of Dentistry and Institute of Oral Bioscience, Jeonju, Korea

<sup>2</sup>Department of Bioengineering, University of Washington, Seattle, WA, USA

<sup>3</sup>Institute for Stem Cell and Regenerative Medicine, University of Washington, Seattle, WA, USA

<sup>4</sup>Center for Cardiovascular Biology, University of Washington, Seattle, WA, USA

<sup>5</sup>Research Institute of Clinical Medicine, Chonbuk National University, Jeonju, Korea

<sup>6</sup>Biomedical Research Institute, Chonbuk National University Hospital, Jeonju, Korea

## OPEN ACCESS

Received: 15 Nov, 2017

Accepted: 23 Dec, 2017

### \*Correspondence:

Jeong-Ho Yun

Department of Periodontology, Chonbuk National University School of Dentistry, 567 Baekje-daero, Deokjin-gu, Jeonju 54907, Korea.  
E-mail: grayheron@hanmail.net  
Tel: +82-63-250-2289  
Fax: +82-63-250-2289

Copyright © 2017. Korean Academy of Periodontology

This is an Open Access article distributed under the terms of the Creative Commons Attribution Non-Commercial License (<https://creativecommons.org/licenses/by-nc/4.0/>).

### ORCID iDs

Joong-Hyun Kim   
<https://orcid.org/0000-0002-2219-2264>  
Seok-Yeong Ko   
<https://orcid.org/0000-0002-0800-1409>  
Justin Ho Lee   
<https://orcid.org/0000-0002-0284-2389>  
Deok-Ho Kim   
<https://orcid.org/0000-0002-6989-6074>  
Jeong-Ho Yun   
<https://orcid.org/0000-0003-3929-4467>

### Funding

This research was supported by a grant of the Korea Health Technology R&D Project through the Korea Health Industry Development

## ABSTRACT

**Purpose:** The aim of this study was to determine the effects of patterned human periodontal ligament stem cell (hPDLSC) sheets fabricated using a thermoresponsive substratum.

**Methods:** In this study, we fabricated patterned hPDLSC sheets using nanotopographical cues to modulate the alignment of the cell sheet.

**Results:** The hPDLSCs showed rapid monolayer formation on various surface pattern widths. Compared to cell sheets grown on flat surfaces, there were no significant differences in cell attachment and growth on the nanopatterned substratum. However, the patterned hPDLSC sheets showed higher periodontal ligamentogenesis-related gene expression in early stages than the unpatterned cell sheets.

**Conclusions:** This experiment confirmed that patterned cell sheets provide flexibility in designing hPDLSC sheets, and that these stem cell sheets may be candidates for application in periodontal regenerative therapy.

**Keywords:** Extracellular matrix; Periodontal ligament; Regeneration; Stem cells; Tissue engineering

## INTRODUCTION

Periodontitis, the sixth most prevalent health condition worldwide, is a common chronic inflammatory disease that results in degradation of the supporting tissues around the teeth, potentially leading to tooth loss if left untreated [1]. Periodontal regeneration, which comprises the regeneration of alveolar bone, periodontal ligament (PDL), and cementum (American Academy of Periodontology, Consensus report, 1996), is considered to be the ultimate goal of periodontal treatment. Despite the success of periodontal surgery with debridement, regeneration induced by surgical treatment is still not fully predictable [2]. Several regenerative treatment modalities, such as root biomodification, bone grafts, guided tissue regeneration, bioactive factors, and combinations thereof, have been proposed,

Institute (KHIDI), funded by the Ministry of Health & Welfare, Republic of Korea (grant number: HI17CO450).

**Author Contributions**

Conceptualization: Jeong-Ho Yun; Formal analysis: Joong-Hyun Kim, Seok-Yeong Ko, Justin H. Lee; Funding acquisition: Jeong-Ho Yun; Investigation: Jeong-Ho Yun, Joong-Hyun Kim; Methodology: Jeong-Ho Yun, Joong-Hyun Kim, Deok-Ho Kim; Project administration: Jeong-Ho Yun; Writing - original draft: Jeong-Ho Yun, Joong-Hyun Kim, Seok-Yeong Ko; Writing - review & editing: Jeong-Ho Yun, Joong-Hyun Kim, Justin H. Lee, Deok-Ho Kim.

**Conflict of Interest**

Joong-Hyun Kim, Seok-Yeong Ko, Justin H. Lee and Jeong-Ho Yun declare no competing financial interests. Deok-Ho Kim is a co-founder and scientific board member at NanoSurface Biomedical Inc.

but the majority of these therapies have shown limited success, especially in challenging clinical situations [3,4]. Thus, alternative materials or techniques that can be combined with periodontal therapy to achieve predictable periodontal regeneration are highly desirable.

Tissue engineering has emerged as a potential alternative to traditional regenerative approaches, and stem cell therapies have played an important role in promoting periodontal regeneration [5]. After stem cells exhibiting self-renewal and multipotent characteristics were isolated from the PDL (periodontal ligament stem cells; PDLSCs), PDLSCs have been proposed as a viable option for periodontal regeneration [6]. Studies have found PDLSCs to exhibit a superior ability compared to bone marrow-derived mesenchymal stem cells (MSCs) to differentiate into not only PDL, but also into alveolar bone and cementum under regenerative conditions [7]. However, existing tissue engineering approaches usually require scaffolds to deliver cell matrix to the target organ. Scaffolds can potentially induce an inflammatory reaction originating from the biodegraded scaffolds [8]. The possibility of inflammatory reactions resulting from biodegradation can be avoided by using cell transplantation without a scaffold [9]. Cell sheet engineering technology using temperature-responsive dishes has been proposed as a means of overcoming this problem of traditional tissue engineering therapy, and has played an increasingly significant role in periodontal regeneration [9,10].

Okano et al. [11] developed a cell sheet manufacturing method to control cell surface adhesion using poly(N-isopropyl-acrylamide) (PNIPAM), a surface-grafted temperature-responsive polymer. Compared to scaffold-based tissue engineering, a cell sheet can deliver robust cells that are connected through intact cell-cell interactions and extracellular matrix (ECM) proteins [12]. Since PNIPAM transforms in response to temperature changes, harvesting cells using this method does not require matrix-digesting enzymes, which can induce cell damage. Cell sheet engineering allows the harvesting of cultured cells with an intact ECM. Preservation of the ECM proteins is a key requirement for the successful utilization of a cell sheet to construct an appropriate extracellular microenvironment for regeneration [13]. Effectively preserved cellular microenvironments, which have the various biological and mechanical properties of ECM, increase the cell survival rate and reduce cell loss during cell sheet implantation [14]. Additionally, cell sheet engineering provides the opportunity for PDLSCs to be delivered directly to the root surface. Maintenance of the integrity of the fibronectin of the cell sheet results in better adherence of the cell sheets to the denuded root surface [5]. Transplantation of cell sheets using PDLSCs has been successfully used to promote periodontal regeneration both in preclinical animal models and in clinical practice [8]. Studies of periodontal regeneration using cell sheet technology have employed sheets of randomly distributed cells. However, the native PDL has a well-organized fiber structure. To arrange the cells, we focused on giving nanotopographical cues to human periodontal ligament stem cells (hPDLSCs) by culturing the cells upon a nanopatterned substrate. Matrix nanotopographical cues have been explored as a way of controlling various behaviors of stem cells, including their adhesion, proliferation, migration, and differentiation [15,16]. Previous studies showed that the physical interaction between nanoscale materials and cells could be used to manipulate the osteogenic differentiation of MSCs, and the function of PDLSCs has been shown to be modulated by the local nanotopography [17,18]. Therefore, by fabricating an aligned hPDLSC sheet, cell morphology and function can be modulated. Jiao et al. [19] developed a thermoresponsive and nanopatterned substratum for the fabrication of patterned cell sheets using PNIPAM. The self-organization of cells in response to the directional cues of the nanotopography

happened quickly (within 2 hours of seeding), enabling the rapid formation of a patterned monolayer. In light of the benefits discussed above, the generation of patterned cell sheets using hPDLSCs may be a next-generation regenerative therapy for periodontitis.

The aim of this study was to develop a favorable method for regenerating periodontal tissue using patterned PDLSC sheets. We hypothesized that the fabrication of patterned hPDLSC-based stem cell sheets using a thermoresponsive substratum would enhance the ability of these stem cells to facilitate periodontal regeneration compared to cell sheets based on a flat surface, thereby providing a new strategy for periodontal therapy.

## MATERIALS AND METHODS

### Preparation of the nanopatterned substratum

The nanopatterned substratum was prepared using capillary force lithography (CFL)-based techniques, as described elsewhere (Figure 1A) [19]. Scaffolds with various nanotopographical cues (parallel ridges and grooves 200-, 400-, 800-, and 1,600-nm wide and 600-nm deep) were fabricated using a photopolymerizable poly(urethane acrylate)-poly(glycidyl methacrylate) composite. In epoxy amine chemistry, amine-terminated PNIPAM covalently binds to surface epoxy groups. Scanning electron microscopy (SEM) analysis was performed to confirm the fidelity of the nanopatterns retained on the surfaces.

### Primary cell culture of hPDLSCs

hPDLSCs were used to form cell sheets on the nanopatterned surfaces. To isolate hPDLSCs, premolars were extracted from healthy patients who visited Chonbuk National University Dental Hospital, Jeonju, Korea. The isolation of the hPDLSCs was approved by the Ethics Committee of Chonbuk National University Hospital (Approval No. CUH 2015-06-038-001). The subjects enrolled in this study provided written informed consent.

Briefly, periodontal tissue samples were obtained from the root surface and were digested using 2 mg/mL of collagenase (Wako Pure Chemical Industries, Tokyo, Japan) and 1 mg/mL of dispase (Gibco, Grand Island, NY, USA). The cells were seeded in a T-75 cell culture flask (BD Falcon Labware, Franklin Lakes, NJ, USA). The normal growth medium (NGM) consisted of alpha minimum essential medium (Gibco), 15% fetal bovine serum (Gibco), 2 mmol/L of L-glutamine (Gibco), 100  $\mu$ mol/L of ascorbic-acid-2-phosphate (Sigma-Aldrich, St. Louis, MO, USA), and a mixture of antibiotics consisting of 100 U/mL of penicillin and 100  $\mu$ g/mL of streptomycin (Gibco). The atmosphere was kept humidified at 37°C with 5% CO<sub>2</sub>, and cells at passages 5 to 8 were used for the following experiments.

### Colony-forming assays using hPDLSCs

Single-cell suspensions of hPDLSCs (passage 2 [P2],  $1 \times 10^2$  cells) were seeded in 100-mm diameter culture dishes in NGM. After 14 days in culture, the cells were fixed with 4% paraformaldehyde (PFA) and stained with crystal violet solution. Cell aggregates larger than 3 mm were counted as colonies, under microscope visualization (Zeiss Axio Scope A1; Carl Zeiss Co., Ltd, Jena, Germany).

### Osteogenic and adipogenic differentiation of hPDLSCs

The osteogenic and adipogenic differentiation of hPDLSCs was confirmed according to methods described in previous reports [20]. Briefly, single-cell suspensions of

hPDLSCs ( $P5$ ,  $2 \times 10^5$  cells) in NGM were seeded in 6-well plates. Upon reaching 80% confluence, the PDLSCs were cultured in osteogenic differentiation medium consisting of NGM supplemented with  $10^{-8}$  mol/L of dexamethasone and 1.8 mmol/L of  $\text{KH}_2\text{PO}_4$ , and in adipogenic medium consisting of NGM supplemented with  $10^{-7}$  mol/L of dexamethasone, 10  $\mu\text{g}/\text{mL}$  of insulin, 0.5  $\mu\text{mol}/\text{L}$  of 1-methyl-3-isobutylxanthine, and 50  $\mu\text{g}/\text{mL}$  of indomethacine. The medium was changed every 3 days. To evaluate osteogenic mineralization and adipogenic lipid formation, the cells were fixed with 4% PFA for 20

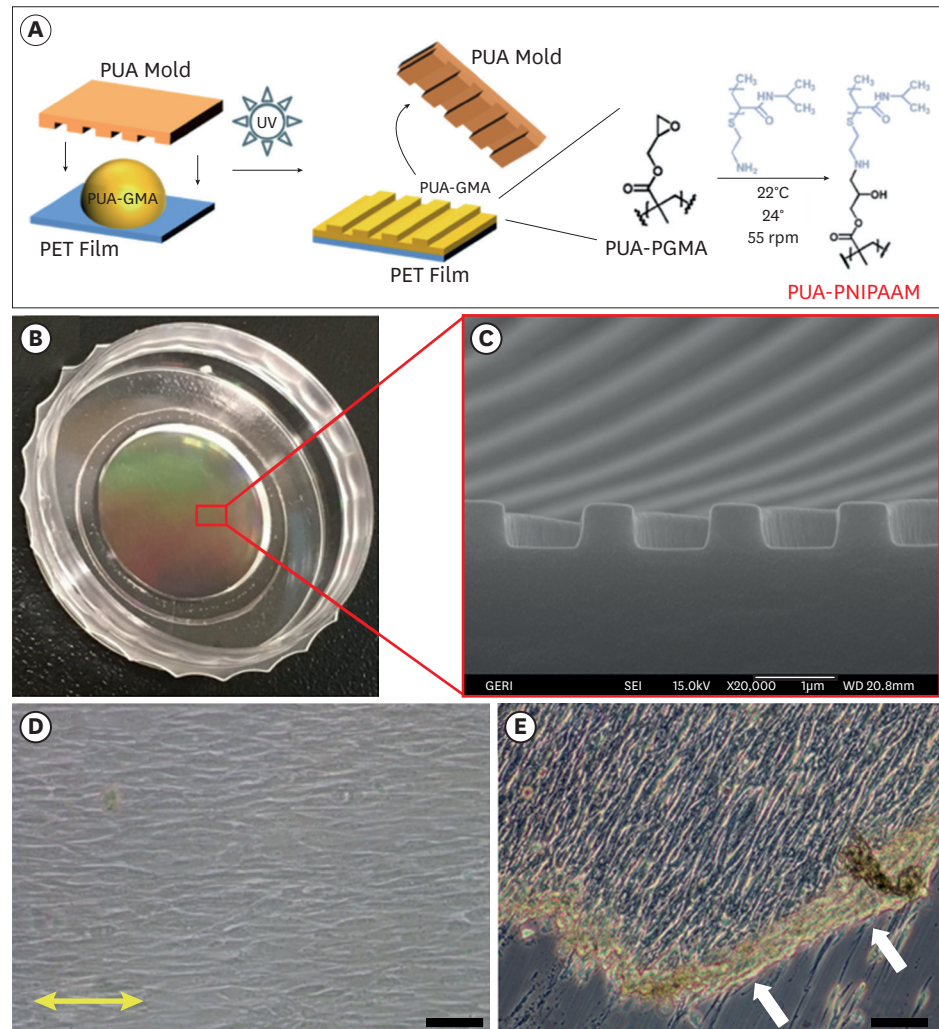


**Figure 1.** (A) The PNIPAM-functionalized thermoresponsive substratum with nanopatterns. Capillary force lithography was used for the fabrication of the substratum, with subsequent modification using amine-terminated PNIPAM on the PET film. (B) Representative macroscopic image of a large-area, scalable substratum, and (C) an SEM image of the 800-nm nanopatterned surface. (D) A microscopic view of hPDLSCs cultured on the 800-nm width nanopatterned surface incubated at 37°C for 48 hours following cell seeding. The yellow arrow designates the direction in which the hPDLSCs were aligned (scale bar=200  $\mu\text{m}$ ). (E) Cell sheet detachment from the substratum after low-temperature treatment. An aligned and interconnected hPDLSC sheet with intact cell-to-cell junctions was slowly detached from the substratum as a single monolayer sheet upon water penetration from the periphery after being maintained at 22°C for 30 minutes. The white arrow indicates the direction of detachment (scale bar=200  $\mu\text{m}$ ).

PNIPAM: poly(N-isopropyl-acrylamide), SEM: scanning electron microscopy, hPDLSC: human periodontal ligament stem cell, PUA: poly(urethane acrylate), GMA: glycidyl methacrylate, PET: poly(ethylene terephthalate), PGMA, poly(glycidyl methacrylate).

minutes and stained with 2% alizarin red-S or oil red O at room temperature. Finally, the cells were observed under light microscopy, using a routine protocol, and photographed.

### Flow-cytometric analysis of the hPDLSC immunophenotyped

hPDLSC surface markers were stained and analyzed by flow cytometry, as described previously [20]. Single-cell suspensions of hPDLSCs ( $P5$ ,  $5 \times 10^5$  cells) were incubated with primary antibodies for human CD19, CD44, CD105, CD146, and stromal cell surface marker-1 (STRO-1) for 1 hour at  $4^\circ\text{C}$ . After 2 washes, the cells were incubated with fluorescein isothiocyanate-conjugated antibodies for CD105, CD146, STRO-1, and CD19, and phycoerythrin-conjugated antibody for CD44 for 30 minutes at  $4^\circ\text{C}$  in the dark. The cells were subjected to flow-cytometric analysis using a Beckman Coulter CytoFLEX (Beckman Coulter, Fullerton, CA, USA). The hematopoietic marker CD19 was used as a negative control.

### hPDLSC patterning

To form a confluent monolayer cell sheet, hPDLSCs were seeded at a high density ( $6.5 \times 10^4$  cells/cm<sup>2</sup>) on flat and nanopatterned surfaces with various-width nanopatterns (200, 400, 800, and 1,600 nm), and allowed to attach for 48 hours at  $37^\circ\text{C}$ . After cell sheet formation, images were obtained using a microscope (CKX41, Olympus, Tokyo, Japan).

To compare the attached cell morphology on the flat surface and an 800-nm-width nanopatterned surface, hPDLSCs ( $3.2 \times 10^3$  cells/cm<sup>2</sup>) were seeded onto each sample type. After 12 hours of incubation, the cells were imaged, and the orientation of the hPDLSCs was analyzed. The orientation angle of a cell with respect to the direction of the surface groove was recorded using image analysis software (Scion Image, National Institutes of Health, Washington, D.C., USA). A  $0^\circ$  angle was parallel to the groove and a  $90^\circ$  angle was perpendicular to the groove. After the orientation angles were determined, the angles were binned into 9 groups representing  $10^\circ$  increments:  $0^\circ$ – $10^\circ$ ,  $11^\circ$ – $20^\circ$ , ...,  $71^\circ$ – $80^\circ$ , and  $81^\circ$ – $90^\circ$ .

### hPDLSC proliferation on the nanopatterned surfaces

To compare cell proliferation on the flat and nanopatterned surfaces, hPDLSCs ( $3.2 \times 10^3$  cells/cm<sup>2</sup>) were seeded on the flat and 800-nm-width nanopatterned surface. The cell proliferation level was quantified using cell counting kit-8 (CCK-8) (Dojindo Molecular Technologies, Inc., Kumamoto, Japan) at 1, 4, 7, and 10 days. The cultured cells were incubated with medium including 10% CCK-8 reagent for 2 hours, and an aliquot from each well (100  $\mu\text{L}$ ) was transferred to a 96-well plate. The absorbance was measured at 450 nm using a multimode microplate reader (SpectraMax PLUS384, Molecular Devices, Sunnyvale, CA, USA), and the reading intensity was interpreted.

### Quantitative real-time polymerase chain reaction (RT-PCR)

After the patterned hPDLSC sheets were formed, they were cultured for 4 or 7 additional days to assess the gene expression associated with periodontal differentiation, which included osteogenic, cementogenic, and ligamentogenic differentiation. Cells cultured on a thermoresponsive flat surface served as a control. Total RNA was extracted from samples using Trizol reagent (Invitrogen, Carlsbad, CA, USA), and cDNA was generated from 2  $\mu\text{g}$  of each RNA sample using GoScript™ Reverse Transcription System (Promega Corporation, Madison, WI, USA). RT-PCR was performed using Power SYBR® Green PCR Master Mix (Applied Biosystems, Foster City, CA, USA) with selected primers. Primer sequences with gene bank accession numbers are shown in Table 1. Experiments were carried out in triplicate for each sample, and RT-PCR experiment was repeated 3 times.

**Table 1.** Primer sequences for quantitative RT-PCR

| Target gene (GenBank No.)      | Direction | Primer sequence      |
|--------------------------------|-----------|----------------------|
| <i>POSTN</i> (AY918092.1)      | Forward   | AATCATCCATGGGAACCAGA |
|                                | Reverse   | GCCTCCAATATGTCCGATGT |
| $\alpha$ -SMA (NM_001141945.1) | Forward   | ACTGGGACGACATGGAAAAG |
|                                | Reverse   | TACATGGCTGGGACATTGAA |
| <i>SCLX</i> (NM_001080514.2)   | Forward   | TCCAGCTACATCTCGCACCT |
|                                | Reverse   | GTTTGGGCTGGGTGTTCTC  |
| <i>OCN</i> (NM_199173.4)       | Forward   | CTCACACTCCTCGCCTATT  |
|                                | Reverse   | TCCCAGCCATTGATACAGGT |
| <i>ALP</i> (XM_006710546.1)    | Forward   | CCACGTCTTCACATTGGTG  |
|                                | Reverse   | AGACTGCGCCTGGTAGTTGT |
| <i>CEMP1</i> (NM_001048212.3)  | Forward   | TGAGAACCTCACCTGCCTCT |
|                                | Reverse   | ATGTGGATCCTGACCTCCTG |
| <i>RUNX2</i> (XM_011514961.1)  | Forward   | TCTGGCCTCCACTCTCAGT  |
|                                | Reverse   | GACTGGCGGGGTGAAGTAA  |
| <i>GAPDH</i> (NM_002046.5)     | Forward   | CAATGACCCCTTCATTGACC |
|                                | Reverse   | TTGATTTGGAGGGATCTCG  |

RT-PCR: real-time polymerase chain reaction, *POSTN*: periostin,  $\alpha$ -SMA:  $\alpha$ -smooth muscle actin, *SCLX*: scleraxis, *OCN*: osteocalcin, *ALP*: alkaline phosphatase, *CEMP1*: cementum protein 1, *RUNX2*: runt-related transcription factor 2, *GAPDH*: glyceraldehyde-3-phosphate dehydrogenase.

### Statistical analysis

Results were expressed as mean±standard deviation. Statistical analyses were performed using SPSS/PC+ version 12.0 for Windows (SPSS Inc., Chicago, IL, USA). The Mann-Whitney test, a non-parametric test, was performed since the Shapiro-Wilk normality test found that the data did not follow a normal distribution ( $P < 0.05$ ). Differences with  $P$  values  $< 0.05$  were considered to be statistically significant.

## RESULTS

### Fabrication of the thermoresponsive nanopatterned substratum

A thermoresponsive nanopatterned substratum, functionalized with CFL-based nanofabrication techniques while preserving the pattern, was successfully fabricated on a culture dish surface (Figure 1A). A representative macroscopic image of a large-area, scalable thermoresponsive substratum (Figure 1B) and an SEM image confirmed the nanopattern fidelity of the substratum (Figure 1C). After incubation on the thermoresponsive substratum at 37°C for 48 hours, hPDLSCs were aligned with the direction of the nanopatterns, and formed well-connected confluent monolayer tissue (Figure 1D). To visualize the thermoresponsive spontaneous detachment, the aligned hPDLSC sheet was incubated in Dulbecco's phosphate-buffered saline at room temperature. Within 20 minutes, the cell sheet began to detach and retract inward from the edges, contracting along the longitudinal axis, and the whole sheet was separated from the substratum (Figure 1E).

### Isolation and characterization of hPDLSCs

The effect of nanotopography on hPDLSC patterning was assessed. The isolated cells formed single colonies (Figure 2A) and exhibited the ability of engage in multi-differentiation when cultured in osteogenic or adipogenic induction media. The formation of mineralized nodules and lipid droplets in the PDLSCs was shown by alizarin red S (Figure 2B) and oil red O (Figure 2C) staining, respectively. The results of a flow-cytometry assay revealed a marker pattern typical for MSCs (positive for CD44, CD105, CD146, and STRO-1 and negative for CD19), indicating that the hPDLSCs contained a stem cell-like population (Figure 2D).

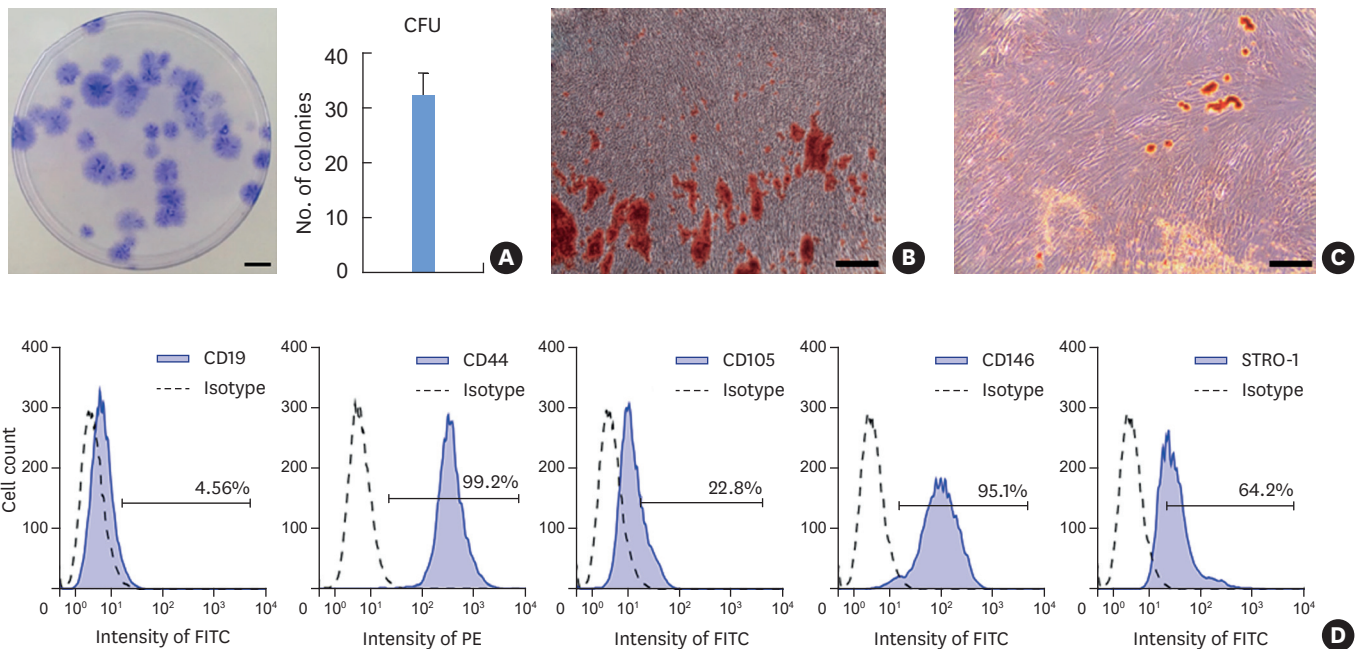


**Figure 2.** Characterization of primary cultured hPDLSCs. (A) Representative images of crystal violet staining of CFUs of primary cultured hPDLSCs at day 14 (scale bars=10 mm) and quantitative measurement of the CFUs ( $32.3 \pm 4.0$ , mean  $\pm$  SD). (B) Representative images of alizarin red staining of mineralized nodules after osteogenic differentiation (scale bar=100  $\mu$ m). (C) Representative images of oil red O staining of lipid-rich vacuoles after adipogenic differentiation (scale bar=100  $\mu$ m). (D) Immunophenotypical analyses of hPDLSCs. CD44, CD105, CD146, and STRO-1 were used as positive markers and CD19 was used as a negative marker.

hPDLSC: human periodontal ligament stem cell, CFU: colony-forming unit, SD: standard deviation, STRO-1: stromal cell surface marker-1, FITC: fluorescein isothiocyanate, PE: phycoerythrin.

### Formation of hPDLSC sheets

Cells were cultured on surfaces containing patterns of various widths (200, 400, 800, and 1,600 nm), and on flat surface culture dishes, which were used as a control. The hPDLSCs demonstrated varying degrees of confluent monolayer formation (Figure 3A). The cells attached randomly in a polygonal shape and showed cytoskeleton extensions in multiple directions on the flat surface. In contrast, on the nanopatterned surface, the cells extended and aligned in the direction of the groove, with a spindle-like shape. All 4 experimental groups showed better monolayer formation with increasing pattern width until a width of 800 nm was reached. The 800-nm pattern showed very well-organized cell monolayer formation. The 1,600-nm pattern also showed aligned cells, but had less confluent monolayers with few cell-cell contacts. The effect of the nanopattern on the initial cellular adhesion angle was quantified (Figure 3B). On the flat surface, the angles were randomly distributed. However, on the nanopatterned surface, the cells aligned almost parallel to the direction of the grooves.

### Proliferation of hPDLSCs on the nanopatterned substratum

The cell proliferation level was evaluated for up to 10 days (Figure 4A). There were no significant differences between the groups. During the quantification of cell proliferation, the effects of the nanopattern on the morphological behavior of hPDLSCs were monitored (Figure 4B). The hPDLSCs showed a typical fibroblast-like appearance with a polygonal shape and grew cytoskeleton extensions in multiple directions on the flat surface. However, on the nanopatterned surface, the cells extended and aligned in the direction of groove orientation with a spindle-like shape, and grew parallel to the direction of the grooves during the culture period.

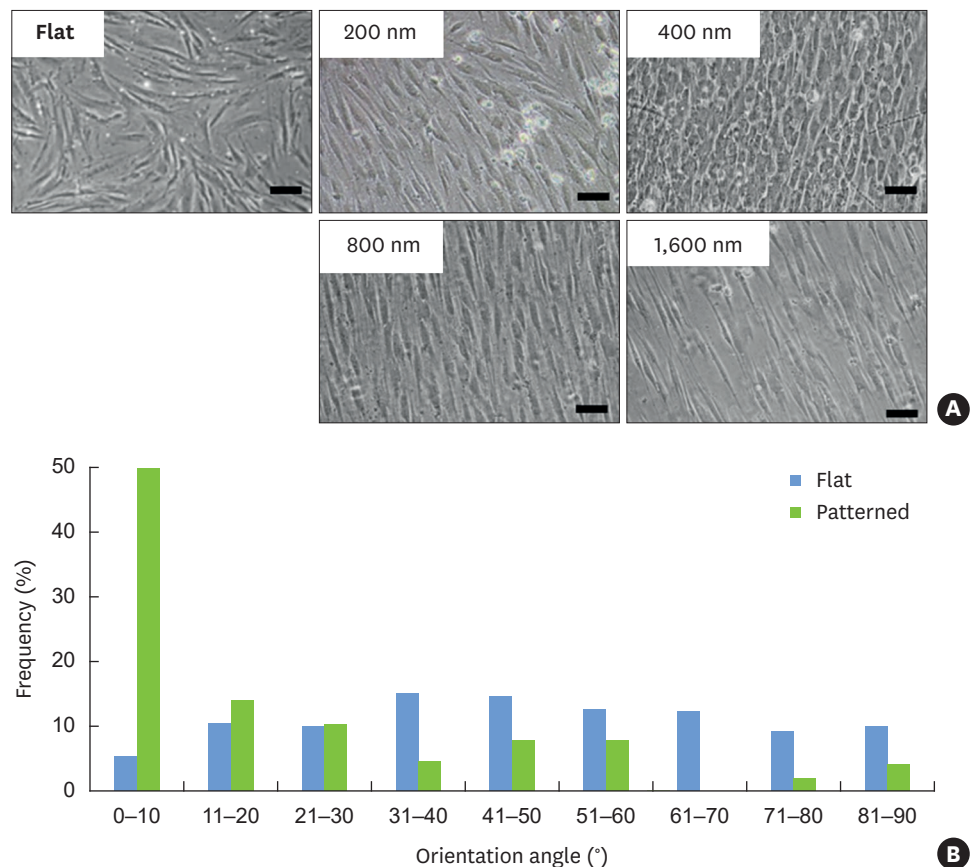


**Figure 3.** Microscopic images of hPDLSC sheet formation from the flat, 200-, 400-, 800-, and 1,600-nm nanopatterns at 48 hours. The hPDLSCs demonstrated varying degrees of confluent cell sheet formation depending on the culture plate surface condition. The 800-nm surface resulted in the optimal conditions for cell patterning (scale bars=200  $\mu$ m). A histogram of the orientation of the hPDLSCs shows the quantified initial cellular adhesion angle on the flat surface and 800-nm width nanopatterned surface. The cells were patterned almost parallel to the direction of the grooves (n=4). hPDLSC: human periodontal ligament stem cell.

### Gene expression in hPDLSCs on the nanopatterned substratum

To determine the effect of nanotopography on the periodontal tissue regenerative capacity of hPDLSCs, differences in periodontal differentiation-related gene expression between flat and nanopatterned surfaces were analyzed using quantitative RT-PCR at early time points (days 4 and 7) (Figure 5). hPDLSCs seeded on nanopatterned surfaces exhibited significant upregulation of the mRNA of the periodontal tissue-specific markers periostin (*POSTN*),  $\alpha$ -smooth muscle actin ( *$\alpha$ -SMA*), and alkaline phosphatase (*ALP*) compared to cells grown on flat surfaces after 7 days of culture in growth medium. Elevated expression of runt-related transcription factor 2 (*RUNX2*) mRNA was noted on both days 4 and 7. There were no significant expression changes in mRNA of cementum protein 1 (*CEMP1*), osteocalcin (*OCN*), or scleraxis (*SCLX*) ( $P < 0.05$ ).

## DISCUSSION

In the present study, we engineered a reproducible hPDLSC sheet using patterned cell sheet engineering technology with a thermoresponsive substratum to improve periodontal

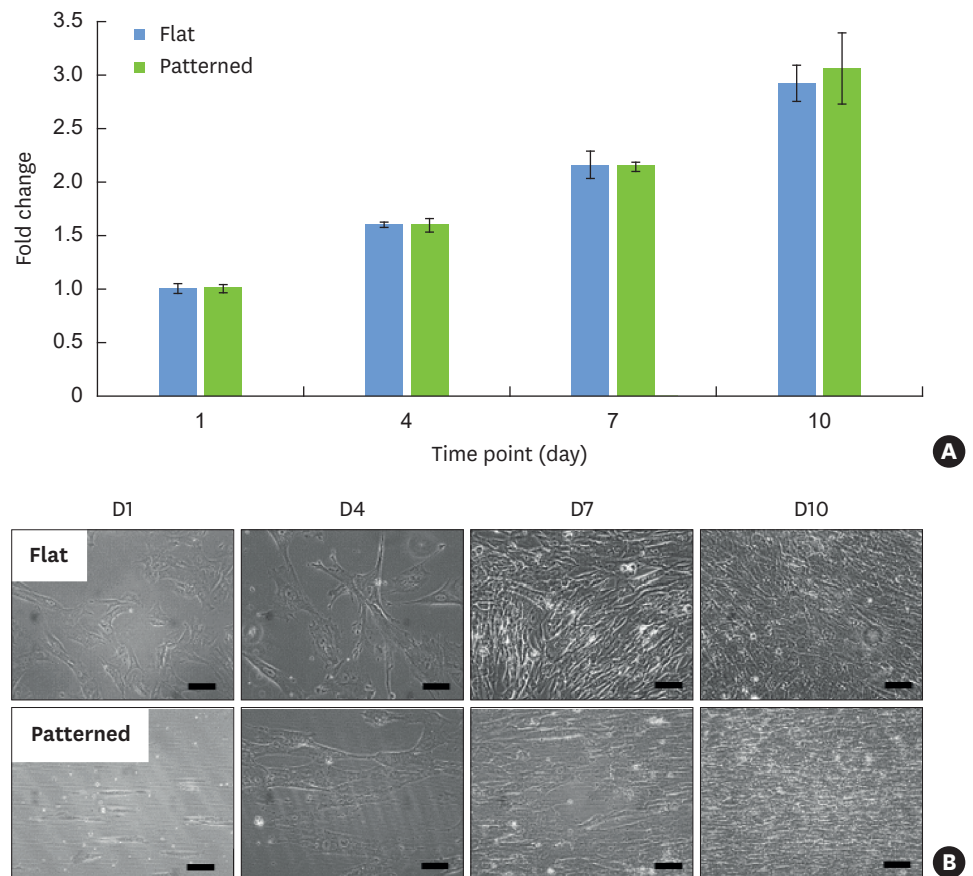


**Figure 4.** Cell proliferation was evaluated for up to 10 days (n=4, P<0.05). Microscopic image sets of cell growth on the flat and nanopatterned surfaces on days 1, 4, 7, and 10. On the nanopatterned surfaces, hPDLSCs extended and patterned in the direction of groove orientation with a spindle-like shape, and grew parallel to the direction of the grooves (scale bars=200  $\mu$ m). hPDLSC: human periodontal ligament stem cell.

tissue regeneration. The ultimate goal of periodontal therapy is to achieve regeneration of the alveolar bone, cementum, and PDL [21]. However, traditional periodontal therapies remain insufficient to achieve complete periodontal regeneration. They arrest the disease process and form a weak attachment, resulting in a condition termed long weak junctional epithelium [22]. Based on recent progress in tissue engineering, *ex vivo* expanded PDLSCs have been used [23]. In this study, we isolated hPDLSCs expressing stem cell surface markers from the root surface for use as cell sources for cell sheet engineering. The expression of CD44 (HCAM), CD105 (endoglin), CD146 (a perivascular cell marker), and STRO-1 (a stem cell marker) indicated that the hPDLSCs used in this study retained their stem cell properties [24]. In particular, cells expressing CD146 are known to be endogenous progenitors that can maintain the homeostasis of the connective attachment underlying the new junctional epithelium [25]. Furthermore, the finding of strong colony formation ability with adipogenic and osteogenic potential demonstrated that hPDLSCs are likely to be a promising candidate for stem cell-mediated periodontal regeneration [26].

In stem cell transplantation for therapeutic purposes, it is important to develop a delivery method that promotes the efficiency of the cells [27]. Traditionally, cell injection therapies have been applied to periodontal bone defects; however, this method has disadvantages,

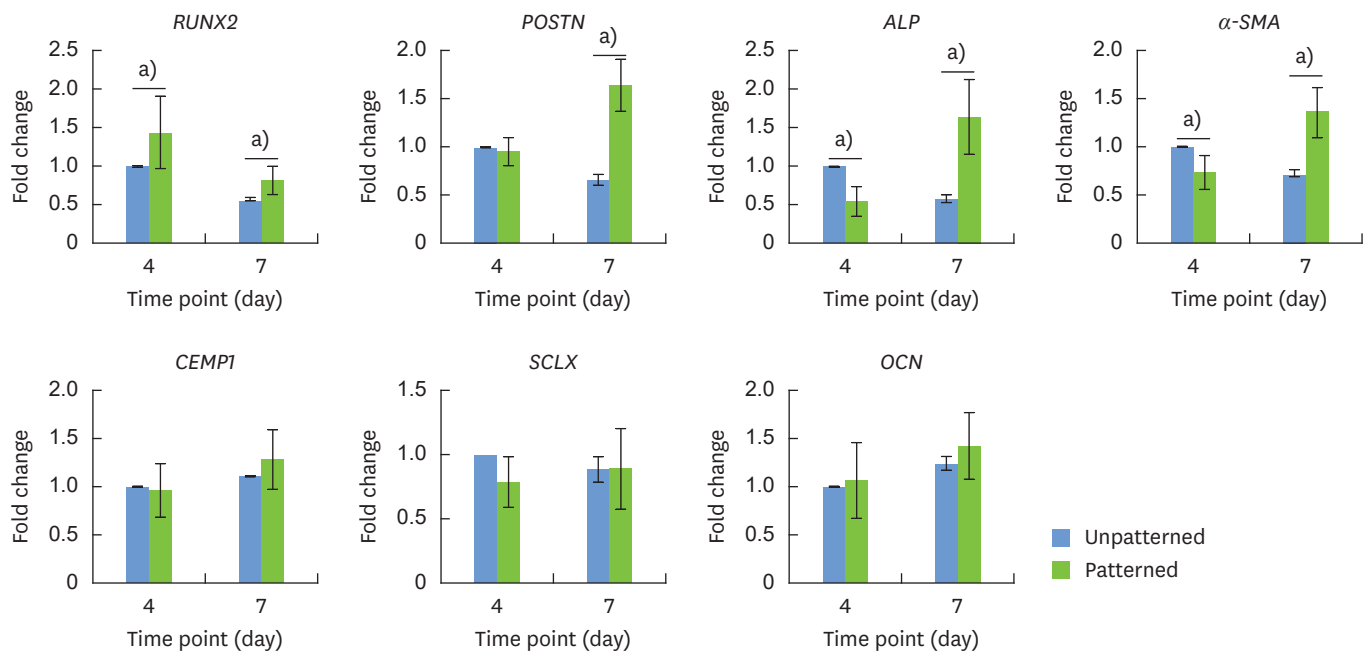


**Figure 5.** Differences in hPDLSC gene expression between patterned and unpatterned cell sheets as assessed by quantitative RT-PCR. The expression of the following genes was upregulated on the patterned cell sheet; *RUNX2* on both days 4 and 7, and *POSTN*, *ALP*, and *α-SMA* on day 7. *α-SMA* and *ALP* showed decreased expression on day 4. There was no significant change in the expression of *CEMP1*, *SCLX*, and *OCN*. hPDLSC: human periodontal ligament stem cell, RT-PCR: real-time polymerase chain reaction, *RUNX2*: runt-related transcription factor 2, *POSTN*: periostin, *ALP*: alkaline phosphatase, *α-SMA*: α-smooth muscle actin, *CEMP1*: cementum protein 1, *SCLX*: scleraxis, *OCN*: osteocalcin. <sup>a)</sup>Statistical significance ( $P < 0.05$ ).

such as a low survival rate, poor engraftment, and unpredictable differentiation under *in vivo* conditions [28]. To avoid these shortcomings, cell sheet technology was designed to provide proper ECM conditions while maintaining differentiated stem cells in the target lineage-specific tissues [29,30]. This technology has been successfully applied to promote periodontal regeneration by delivering cultured cells with an intact ECM [8]. Randomly oriented cell sheets have previously been used. However, in this study, we evaluated the possibility of using a patterned hPDLSC sheet for periodontal regeneration. Nanotopographical cues, consisting of parallel ridges and grooves 200-, 400-, 800-, and 1,600-nm wide and 600-nm deep, were fabricated to modulate the alignment of the hPDLSC sheet. PDL tissue has a highly organized ECM with collagenous fibers. The effect of the nanotopography on patterning PDLSCs enhances the subsequent matrix synthesis and promotes differentiation, which can be a powerful approach as a periodontal therapeutic [31]. A previous study by Jiang et al. [32] demonstrated that by mimicking the natural state of the PDL structure, the aligned PDLSCs improved the expression of collagen type I, which contributes to maturation and mechanical stability, and collagen type III, which presents during the early phase of wound healing, as well as enhancing the expression of *POSTN*, a matricellular protein that plays a role in collagen cross-linking. Consequently, patterning PDLSCs can upregulate the stability and maturation of the PDL during the wound healing process. To fabricate a cell sheet with biomimetic geometry, nanopatterns of various widths were compared to each other. Each nanopattern displayed a different cell morphology and alignment (Figure 3A). This result indicates that hPDLSCs are sensitive to nanoscale topographic cues, and the nanotopography affected cell adhesion and alignment [19]. Additionally, these results demonstrate that the patterning of a cell sheet can be controlled by modifying the nanoscale topography of the substratum (Figure 3B).

To determine the proliferative effect of the nanotopographical changes of the substratum, hPDLSCs were cultured on a nanopatterned surface with grooves that were 800-nm wide and 600-nm deep, and the proliferation level was monitored on days 1, 4, 7, and 10 (Figure 4A). hPDLSCs are known to expand and retract their cytoplasm depending on what they sense in the surrounding environment [33]. When grown on a flat surface, the cells had multiple widely spread cytoskeletal extensions, but when grown on the nanopatterned surface, the hPDLSCs were aligned along the nanopatterns (Figure 4B). It has previously been shown that the nanopattern on the substrate did not interfere with or limit the growth of hPDLSCs, and consequently no variability in cell proliferation by degree of alignment was observed [19]. The substrate topology, which affects the orientation of PDL cells, has been reported to play an important role in maintaining a balanced metabolism between hard and soft tissue turnover during PDL cell differentiation [34]. These findings indicate that our results, with respect to the periodontal regenerative effects of the patterned cell sheets, were not affected by variation in overall cell growth.

In the present study, we also investigated the expression of genes associated with periodontal differentiation to determine the potential effects of hPDLSC patterning while forming a cell sheet (Figure 5). The expression of genes coding for ligamentogenic (*POSTN*, *α-SMA*, and *SCLX*) and osteogenic and cementogenic proteins (*RUNX2*, *ALP*, *OCN*, and *CEMP1*) was evaluated to quantify the characteristics of the resultant cell sheets. Patterned and unpatterned hPDLSC sheets exhibited different mRNA expression profiles after the formation of cell sheets. The expression of ligamentogenic genes tended to increase after patterned cell sheet formation. Nanotopography influenced the differentiation behaviors of the hPDLSCs, and resulted in advantageous periodontal gene expression relative to the control group. Our present findings revealed upregulation of periodontal ligamentogenesis genes (*POSTN* and *α-SMA* at day 7) in hPDLSCs when cultured on the nanopatterned surface. *POSTN*, which is an essential factor for tissue integrity and maturation, modulates PDL homeostasis by promoting the formation of highly stiff collagen [14]. *POSTN* is intensively localized on the Sharpey's fibers, which are essential for dispersing the mechanical forces loaded on the PDL [18]. It has been demonstrated that *α-SMA*-expressing cells from the perivascular regions of the PDL can differentiate into osteoblasts, cementoblasts, and fibroblasts [35]. However, *α-SMA* is less highly expressed in mineralized areas, and is not expressed in fully differentiated cells of the osteoblast lineage [36]. These results revealed that nanotopography influenced the early gene expression of the hPDLSC sheet, especially with respect to PDL formation.

The expression of genes for osteogenic proteins (*ALP* and *RUNX2*) was upregulated in the patterned hPDLSC sheet. Both genes are known to be expressed during osteogenic and cementogenic differentiation [37]. *ALP*, an early marker for osteogenic differentiation, plays a role in bone matrix mineralization through regulation of the Wnt signaling pathway [38]. Upregulation of *ALP* means that the fabricated patterned cell sheet would promote the osteogenic and cementogenic induction potential of hPDLSCs. *RUNX2* is essential for initiating osteogenesis and cementogenesis [39]. Upregulation of *RUNX2* indicates that cementogenic and osteogenic induction was promoted in the patterned hPDLSC sheets. The expression of other genes related to hard tissue maturation (*OCN* and *CEMP1*) and tendon attachment (*SCLX*) were not upregulated. mRNA of *OCN*, a late indicator of osteoblast differentiation, and *CEMP1*, an indicator of cementoblast differentiation, were not upregulated until day 7. As a tendon-specific transcription factor, *SCLX* is required for the formation and maturation of tendons. *SCLX* is modulated by mechanical forces in tendons *in vivo* and *in vitro* [40]. Consequently, the patterned hPDLSC sheet did not upregulate genes

associated with periodontal tissue maturation in the absence of an osteogenic supplement. Most periodontal regeneration studies have focused on osteogenic induction, whereas this study focused on the advantages of patterned hPDLSC sheets for both periodontal osteogenic and ligamentogenic induction, which contribute to the regeneration of periodontal tissue [38]. The results of this study may indicate that nanotopography-induced patterning of the hPDLSC sheet has significant implications for improving the early periodontal tissue formation potential. Additionally, the microenvironment provided by the patterned hPDLSC sheet could provide optimal conditions for periodontal tissue regeneration. More complicated conditions may be needed to study periodontal tissue maturation. For instance, the retention of the nanotopography-induced maturation of hPDLSCs after sheet transfer will still need to be investigated. However, a previous study showed that patterned morphological phenotypes were retained even after cell sheet transfer, which implies that the phenotypical changes induced by nanotopography might be retained after becoming scaffold-free [19].

In conclusion, a nanopatterned substratum functionalized with thermoresponsive polymers facilitated the reproducible and robust fabrication of patterned cell sheets using hPDLSCs. The hPDLSCs showed rapid and spontaneous monolayer formation, as well as improved gene expression patterns related to PDL tissue regeneration compared to the control group. Based on these results, methods of forming cell sheets using a thermoresponsive and nanopatterned substratum could be utilized for the facile and reproducible fabrication of controllable structures. Patterning PDLSCs while fabricating cell sheets would be advantageous for improving periodontal regenerative function.

## REFERENCES

1. Armitage GC. Development of a classification system for periodontal diseases and conditions. *Ann Periodontol* 1999;4:1-6.  
[PUBMED](#) | [CROSSREF](#)
2. Apicella A, Heunemann P, Dejace L, Marascio M, Plummer CJ, Fischer P. Scaffold requirements for periodontal regeneration with enamel matrix derivative proteins. *Colloids Surf B Biointerfaces* 2017;156:221-6.  
[PUBMED](#) | [CROSSREF](#)
3. Reynolds MA, Kao RT, Camargo PM, Caton JG, Clem DS, Fiorellini JP, et al. Periodontal regeneration - intrabony defects: a consensus report from the AAP Regeneration Workshop. *J Periodontol* 2015;86:S105-7.  
[PUBMED](#) | [CROSSREF](#)
4. Greenwell HCommittee on Research, Science and Therapy. American Academy of Periodontology. Position paper: guidelines for periodontal therapy. *J Periodontol* 2001;72:1624-8.  
[PUBMED](#) | [CROSSREF](#)
5. Hasegawa M, Yamato M, Kikuchi A, Okano T, Ishikawa I. Human periodontal ligament cell sheets can regenerate periodontal ligament tissue in an athymic rat model. *Tissue Eng* 2005;11:469-78.  
[PUBMED](#) | [CROSSREF](#)
6. Bright R, Hynes K, Gronthos S, Bartold PM. Periodontal ligament-derived cells for periodontal regeneration in animal models: a systematic review. *J Periodontol Res* 2015;50:160-72.  
[PUBMED](#) | [CROSSREF](#)
7. Gay IC, Chen S, MacDougall M. Isolation and characterization of multipotent human periodontal ligament stem cells. *Orthod Craniofac Res* 2007;10:149-60.  
[PUBMED](#) | [CROSSREF](#)
8. Ishikawa I, Iwata T, Washio K, Okano T, Nagasawa T, Iwasaki K, et al. Cell sheet engineering and other novel cell-based approaches to periodontal regeneration. *Periodontol 2000* 2009;51:220-38.  
[PUBMED](#) | [CROSSREF](#)
9. Xu Q, Li B, Yuan L, Dong Z, Zhang H, Wang H, et al. Combination of platelet-rich plasma within periodontal ligament stem cell sheets enhances cell differentiation and matrix production. *J Tissue Eng Regen Med* 2017;11:627-36.  
[PUBMED](#) | [CROSSREF](#)

10. Carter SD, Costa PF, Vaquette C, Ivanovski S, Hutmacher DW, Malda J. Additive biomanufacturing: an advanced approach for periodontal tissue regeneration. *Ann Biomed Eng* 2017;45:12-22.  
[PUBMED](#) | [CROSSREF](#)
11. Okano T, Bae YH, Jacobs H, Kim SW. Thermally on-off switching polymers for drug permeation and release. *J Control Release* 1990;11:255-65.  
[CROSSREF](#)
12. Li M, Feng C, Gu X, He Q, Wei F. Effect of cryopreservation on proliferation and differentiation of periodontal ligament stem cell sheets. *Stem Cell Res Ther* 2017;8:77.  
[PUBMED](#) | [CROSSREF](#)
13. Guo S, Kang J, Ji B, Guo W, Ding Y, Wu Y, et al. Periodontal-derived mesenchymal cell sheets promote periodontal regeneration in inflammatory microenvironment. *Tissue Eng Part A* 2017;23:585-96.  
[PUBMED](#) | [CROSSREF](#)
14. Wang Z, Feng Z, Wu G, Bai S, Dong Y, Zhao Y. *In vitro* studies on human periodontal ligament stem cell sheets enhanced by enamel matrix derivative. *Colloids Surf B Biointerfaces* 2016;141:102-11.  
[PUBMED](#) | [CROSSREF](#)
15. Dalby MJ, Gadegaard N, Tare R, Andar A, Riehle MO, Herzyk P, et al. The control of human mesenchymal cell differentiation using nanoscale symmetry and disorder. *Nat Mater* 2007;6:997-1003.  
[PUBMED](#) | [CROSSREF](#)
16. Kim DH, Provenzano PP, Smith CL, Levchenko A. Matrix nanotopography as a regulator of cell function. *J Cell Biol* 2012;197:351-60.  
[PUBMED](#) | [CROSSREF](#)
17. McMurray RJ, Gadegaard N, Tsimbouri PM, Burgess KV, McNamara LE, Tare R, et al. Nanoscale surfaces for the long-term maintenance of mesenchymal stem cell phenotype and multipotency. *Nat Mater* 2011;10:637-44.  
[PUBMED](#) | [CROSSREF](#)
18. Gao H, Li B, Zhao L, Jin Y. Influence of nanotopography on periodontal ligament stem cell functions and cell sheet based periodontal regeneration. *Int J Nanomedicine* 2015;10:4009-27.  
[PUBMED](#)
19. Jiao A, Trosper NE, Yang HS, Kim J, Tsui JH, Frankel SD, et al. Thermoresponsive nanofabricated substratum for the engineering of three-dimensional tissues with layer-by-layer architectural control. *ACS Nano* 2014;8:4430-9.  
[PUBMED](#) | [CROSSREF](#)
20. Kim K, Yi T, Yun JH. Maintained stemness of human periodontal ligament stem cells isolated after prolonged storage of extracted teeth. *J Periodontol* 2016;87:e148-58.  
[PUBMED](#) | [CROSSREF](#)
21. Farag A, Vaquette C, Theodoropoulos C, Hamlet SM, Hutmacher DW, Ivanovski S. Decellularized periodontal ligament cell sheets with recellularization potential. *J Dent Res* 2014;93:1313-9.  
[PUBMED](#) | [CROSSREF](#)
22. Hu J, Cao Y, Xie Y, Wang H, Fan Z, Wang J, et al. Periodontal regeneration in swine after cell injection and cell sheet transplantation of human dental pulp stem cells following good manufacturing practice. *Stem Cell Res Ther* 2016;7:130.  
[PUBMED](#) | [CROSSREF](#)
23. Dan H, Vaquette C, Fisher AG, Hamlet SM, Xiao Y, Hutmacher DW, et al. The influence of cellular source on periodontal regeneration using calcium phosphate coated polycaprolactone scaffold supported cell sheets. *Biomaterials* 2014;35:113-22.  
[PUBMED](#) | [CROSSREF](#)
24. Seo BM, Miura M, Gronthos S, Bartold PM, Batouli S, Brahimi J, et al. Investigation of multipotent postnatal stem cells from human periodontal ligament. *Lancet* 2004;364:149-55.  
[PUBMED](#) | [CROSSREF](#)
25. Lemaitre M, Monsarrat P, Blasco-Baque V, Loubières P, Burcelin R, Casteilla L, et al. Periodontal tissue regeneration using syngeneic adipose-derived stromal cells in a mouse model. *Stem Cells Transl Med* 2017;6:656-65.  
[PUBMED](#) | [CROSSREF](#)
26. Wang ZS, Feng ZH, Wu GF, Bai SZ, Dong Y, Chen FM, et al. The use of platelet-rich fibrin combined with periodontal ligament and jaw bone mesenchymal stem cell sheets for periodontal tissue engineering. *Sci Rep* 2016;6:28126.  
[PUBMED](#) | [CROSSREF](#)
27. Feng R, Lengner C. Application of stem cell technology in dental regenerative medicine. *Adv Wound Care (New Rochelle)* 2013;2:296-305.  
[PUBMED](#) | [CROSSREF](#)

28. Du J, Shan Z, Ma P, Wang S, Fan Z. Allogeneic bone marrow mesenchymal stem cell transplantation for periodontal regeneration. *J Dent Res* 2014;93:183-8.  
[PUBMED](#) | [CROSSREF](#)
29. Owaki T, Shimizu T, Yamato M, Okano T. Cell sheet engineering for regenerative medicine: current challenges and strategies. *Biotechnol J* 2014;9:904-14.  
[PUBMED](#) | [CROSSREF](#)
30. Kim JH, Kang MS, Eltohamy M, Kim TH, Kim HW. Dynamic mechanical and nanofibrous topological combinatory cues designed for periodontal ligament engineering. *PLoS One* 2016;11:e0149967.  
[PUBMED](#) | [CROSSREF](#)
31. Yin Z, Chen X, Chen JL, Shen WL, Hieu Nguyen TM, Gao L, et al. The regulation of tendon stem cell differentiation by the alignment of nanofibers. *Biomaterials* 2010;31:2163-75.  
[PUBMED](#) | [CROSSREF](#)
32. Jiang W, Li L, Zhang D, Huang S, Jing Z, Wu Y, et al. Incorporation of aligned PCL-PEG nanofibers into porous chitosan scaffolds improved the orientation of collagen fibers in regenerated periodontium. *Acta Biomater* 2015;25:240-52.  
[PUBMED](#) | [CROSSREF](#)
33. Gauvin R, Parenteau-Bareil R, Larouche D, Marcoux H, Bisson F, Bonnet A, et al. Dynamic mechanical stimulations induce anisotropy and improve the tensile properties of engineered tissues produced without exogenous scaffolding. *Acta Biomater* 2011;7:3294-301.  
[PUBMED](#) | [CROSSREF](#)
34. Yu N, Prodanov L, te Riet J, Yang F, Walboomers XF, Jansen JA. Regulation of periodontal ligament cell behavior by cyclic mechanical loading and substrate nanotexture. *J Periodontol* 2013;84:1504-13.  
[PUBMED](#) | [CROSSREF](#)
35. San Miguel SM, Fatahi MR, Li H, Igwe JC, Aguila HL, Kalajzic I. Defining a visual marker of osteoprogenitor cells within the periodontium. *J Periodontal Res* 2010;45:60-70.  
[PUBMED](#) | [CROSSREF](#)
36. Kalajzic Z, Li H, Wang LP, Jiang X, Lamothe K, Adams DJ, et al. Use of an alpha-smooth muscle actin GFP reporter to identify an osteoprogenitor population. *Bone* 2008;43:501-10.  
[PUBMED](#) | [CROSSREF](#)
37. Jin H, Choung HW, Lim KT, Jin B, Jin C, Chung JH, et al. Recombinant human plasminogen activator inhibitor-1 promotes cementogenic differentiation of human periodontal ligament stem cells. *Tissue Eng Part A* 2015;21:2817-28.  
[PUBMED](#) | [CROSSREF](#)
38. Zhu B, Liu W, Liu Y, Zhao X, Zhang H, Luo Z, et al. Jawbone microenvironment promotes periodontium regeneration by regulating the function of periodontal ligament stem cells. *Sci Rep* 2017;7:40088.  
[PUBMED](#) | [CROSSREF](#)
39. Kadkhoda Z, Safarpour A, Azmoodeh F, Adibi S, Khoshzaban A, Bahrami N. Histopathological comparison between bone marrow- and periodontium-derived stem cells for bone regeneration in rabbit calvaria. *Int J Organ Transplant Med* 2016;7:9-18.  
[PUBMED](#)
40. Scott A, Danielson P, Abraham T, Fong G, Sampaio AV, Underhill TM. Mechanical force modulates scleraxis expression in bioartificial tendons. *J Musculoskelet Neuronal Interact* 2011;11:124-32.  
[PUBMED](#)